Finite Element Analysis of a Stewart Platform using Flexible Joints

Mohd. Furqan
Mechanical Engineering Department
COE, TMU
Moradabad, India
mfurqanamu2006@gmail.com

Dr. Md. Naushad Alam
Mechanical Engineering Department
ZHCET, AMU
Aligarh, India
naushad7863@rediffmail.com

***Abstract*— The demand of high precision motion has been increasing in the recent years. Since performance of today's many mechanical systems requires high stiffness and accurate positioning capability, parallel manipulators gained popularity. Their superior architecture provides better load capacity and positioning accuracy over the serial ones. In this work, a popular parallel manipulator, Stewart Platform, has been studied. Stewart Platform is a positioning system that consists of top plate (moving platform), a bottom plate (fixed base), and six extensible legs connecting the top plate to the bottom plate. This work includes design and analysis of a complete positioning system. In order to achieve better accuracy over commonly used universal and spherical joints the flexible joints have been employed. Flexible joints would give better results than universal and spherical joints because they eliminate friction and backlash. Flexible joint has been developed in the FE software ANSYS for static and modal analysis and using this flexible joint Stewart Platform has been developed in the FE software for FE analysis. The static and modal analysis of the Stewart Platform using flexible joints will be evaluated.**

Keywords*— *stewart platform; flexible joint; finite element analysis

I. INTRODUCTION

Mechanically assembled joints such as universal or ball joints reduce the accuracy due to manufacturing errors. The monolithic characteristics of the flexible joints help avoid manufacturing errors. This characteristic brings easy manufacturing process and implies a very compact design that can be used in the micro-assembly workstation presented in [1-2]. From operation point of view, flexible joints clearly reduce frictional losses. Therefore, they do not require lubrication, and inaccuracies due to lubrication would be eliminated. Flexible joints must be designed extremely carefully due to their very sensitive force-displacement relationship. Because of this, high dimensional accuracy during the fabrication and calibration after fabrication process are needed. Flexure may also be sensitive to the working temperature [3]. The main difference between flexure mechanisms and conventional joints is the consideration of kinematics stability and the design issue. Wei et al. [4] stated that the flexure hinges have a lot of advantages compared to the others such as ball joints or universal ones. Because of the fact that they are manufactured monolithically, they are very compact in structurally. Besides, they have a lot of advantages like having no backlash, no friction, no lubrication and no error due to lubrication. However, they have a limited range of motion as they have to flex without sustaining any plastic deformation at the joints. Flexure hinges with single-axis can be divided into two main categories: leaf and notch type hinges [5]. Due to relative low rotation precision and stress concentration, leaf type hinge is seldom adopted. In 1965, Paros and Weisbord [6] introduced the first notch hinge and circular flexure hinge. The common feature of these two types is ease of manufacture. Therefore, researchers turned their attention to other configurations that could provide precision rotation in an even larger angular range. Smith et al. [7] presented a flexure hinge of elliptic cross-section, the geometry of which is determined by ratio of the major and minor axes. Likewise, Lobontiu et al. [8] introduced an analytical model for corner-filleted flexure hinges that are incorporated into planar amplification mechanisms. Later, they also introduced the parabolic and hyperbolic hinges configurations [9]. Closed-form equations are formulated to characterize their compliance both for the active rotation and all other in and out-of-plane motions. To sum up, Gui-Min et al. [5] represented the compliance model or the right circular hybrid flexure hinges. The close-form solutions were provided to characterize the flexibility and precision of rotation. The precision model with stress considerations were verified with the finite element analysis. Their results show that the most suitable solutions for large displacements and high accuracy are reached with the right circular hybrid flexure hinges rather than the right circular ones and corner filleted hinges. According to Lobontiu and Garcia [10], the flexure needs to be compliant in the bending direction and rigid for all other axes and deformations. Constructively, a flexure hinge may have several sensitive axes. These sensitive axes define the rotations and motions. Apart from these, Paros and Weisbord [6] presented two-axis circular flexure hinges which are designed in serial configuration. The serial design preserves the convenience of having each flexure hinge designed according to the standard-axis geometry. However, it also requires the extra-length that is necessary to locate the two flexures in a serial manner.

II. FLEXIBLE JOINT

Flexible joints as the main part of the system are studies considering different profile of the flexible joints and effective design parameter to introduce the best profile of the joints based on the application that is needed. For this purpose five different profiles (right circular, elliptical, corner-filleted, hyperbolic and parabolic) of flexible joints have been considered and further studies have been carried out on flexible joints based on some parameters such as accuracy, flexibility and the maximum stress in the joints.

In order to study the accuracy of flexure hinge, an FE model is created in ANSYS (FE Software) in which the material used is steel (E = 207E9, υ = 0.3) "Fig. 2," The displacement of the flexure hinge rotation center produced by input displacement of 0.1 mm applied at the right edge indicates the accuracy of the flexure hinge. Whatever this displacement was smaller the flexure hinge operates closer to a real hinge.

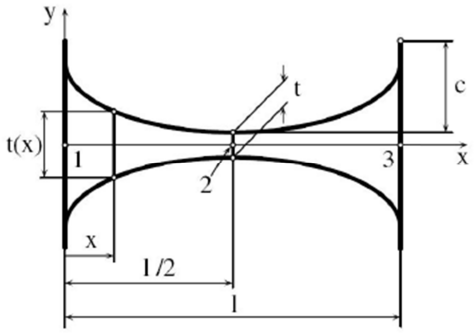

Fig. 1. Parameters defining a symmetric conic-section flexure hinge

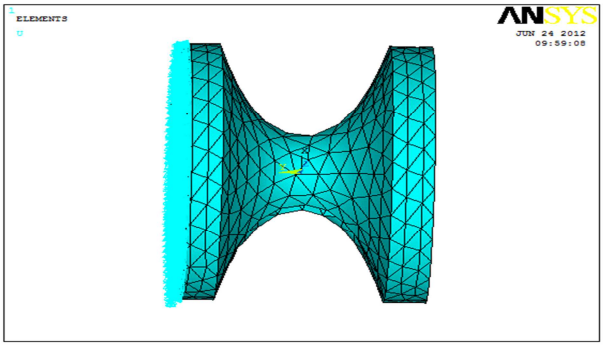

Fig. 2. Parametric design of a flexure hinge

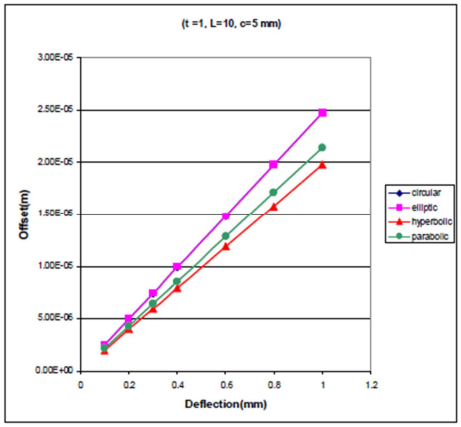

Fig. 3. Geometric corner's offset for different flexure profile

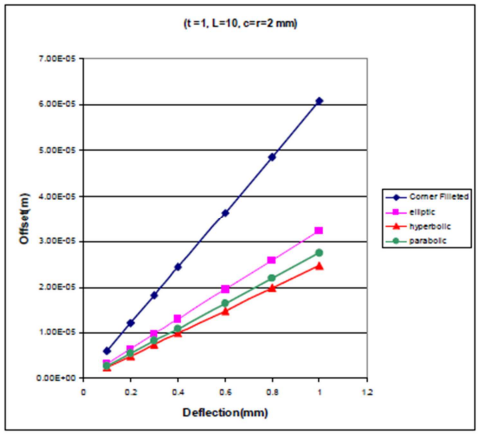

Fig. 4. Geometric corner's offset vs. end deflection for different flexure profile

From the "Fig. 3," and "Fig. 4," we can observe that as the deflection increases the geometric corner's offset increase in a large amount for Corner-Filleted flexure hinge than for Elliptical flexure hinge than for Parabolic flexure hinge and in least amount for Hyperbolic flexure hinge. So "Fig. 3," and "Fig. 4," shows that hyperbolic flexure hinge is the most accurate profile and Corner-Filleted flexure hinge is the least accurate profile.

A. *Modelling of Hyperbolic Flexible Joint*

Considering the flexure hinge geometric specifications of $t = 10$, $l = 100\,mm$ and the property taken into account for the Titanium material as: Modulus of Elasticity (N/mm^2) = 109872, Poission Ratio = 0.3, Density (kg/m^3) = 4500, Yield strength (N/mm^2) = 1345. After considering above parameters, the flexure joint is developed in ANSYS software is shown in "Fig. 5,".

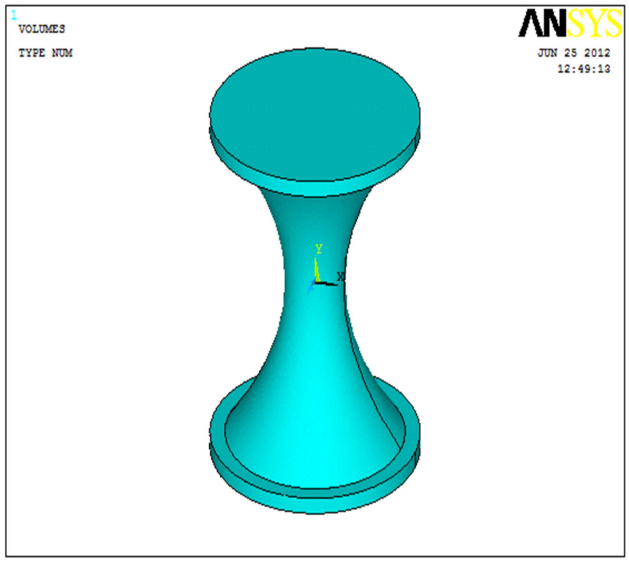

Fig. 5. Solid model of hyperbolic flexure joint

B. *Static Stress Analysis*

The mashed part with solid element and taking 20node186 3D element and created 1325 element with the shape of the element is tetragonal within the volume of the solid model with free mesh is shown in "Fig. 6,".

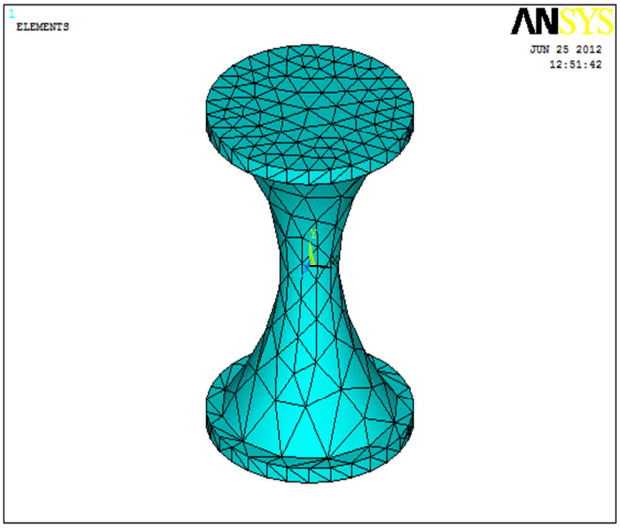

Fig. 6. Model with Meshed region

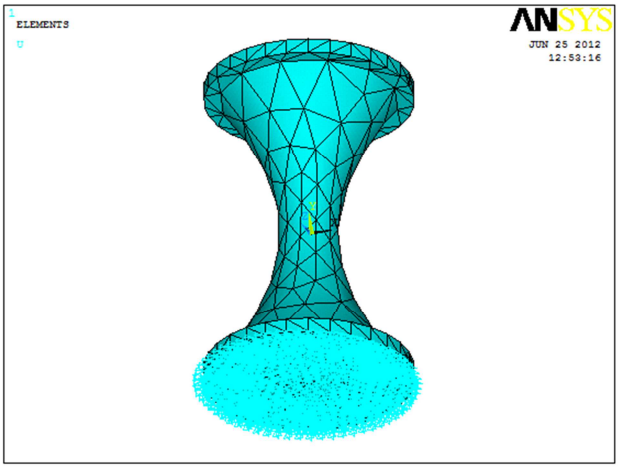

Fig. 7. Model with Boundary condition

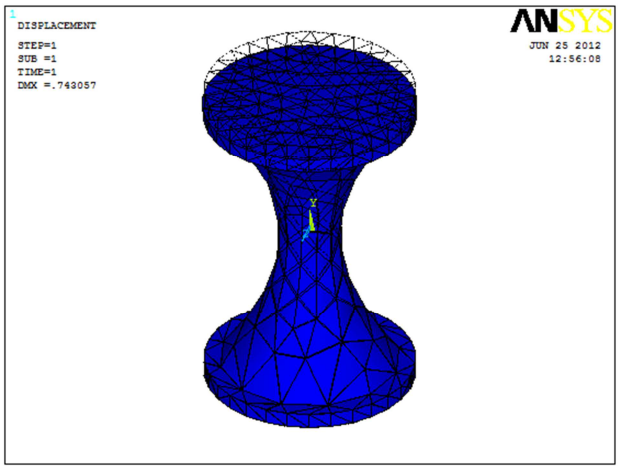

Fig. 8. Undeformed and deformed shape of the flexure joint

The boundary condition is applied to the flexural hinge structure at the bottom as it is attached to the fixed base so the geometry at the bottom is fixed i. e. encaster to prevent a relative motion and is shown in "Fig. 7," The load is applied to the upper face. "Fig. 8," shows the undeformed and deformed shape of the flexure joint. The stress for different values of flexure thickness and length is given in Table I and in Table II.

Table I. Maximum stress for different values of flexure thickness

S. No.	Flexure Thickness (t) mm	Maximum Stress (N/mm^2)
1	6	2169.91
2	8	1994.97
3	10	1273.46
4	12	895.81
5	14	645.62
6	16	493.89

Table II. Maximum stress for different values of flexure length

S. No.	Flexure Length (l) mm	Maximum Stress (N/mm^2)
1	60	1453.77
2	80	1352.65
3	100	1309.01
4	120	1297.45
5	140	1295.59
6	160	1269.41

From the above static stress analysis, we have analyzed the stress pattern throughout the model. "Fig. 9," shows the maximum stress developed in the model for flexure thickness t = 10 mm is 1273.46 N/mm^2 and "Fig. 10," shows the maximum stress developed in the model for flexure length l = 100 mm is 1309.01 N/mm^2 which are less than the Titanium material Yield strength = 1345 N/mm^2. So t = 10 mm and l = 100 mm are the design parameter for the flexure joint.

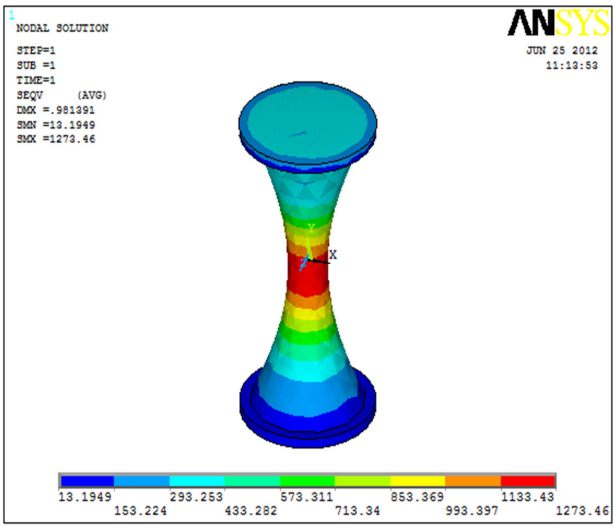

Fig. 9. Stress pattern for flexure thickness t = 10 mm

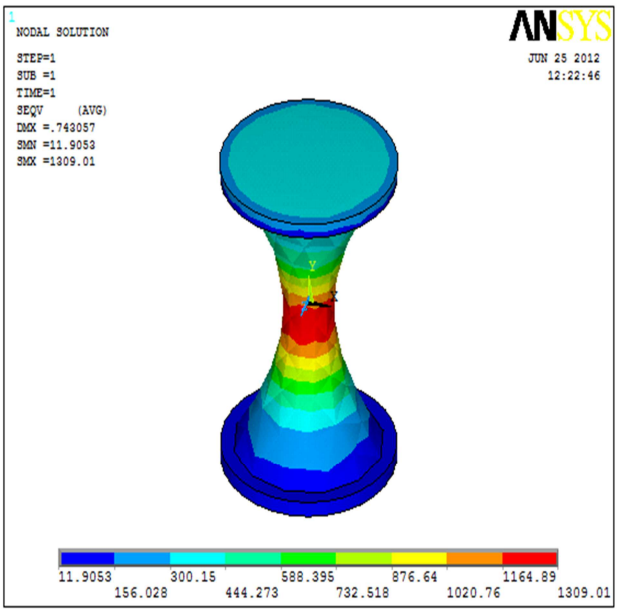

Fig. 10. Stress pattern for flexure length l = 100 mm

III. STEWART PLATFORM

A. *Modelling of Stewart Platform*

For the modelling of Stewart Platform using the flexure joint considering the following design parameters [16]. After considering these parameters the solid model of Stewart Platform with flexure joint is generated in the ANSYS software and is shown in “Fig. 11,”.

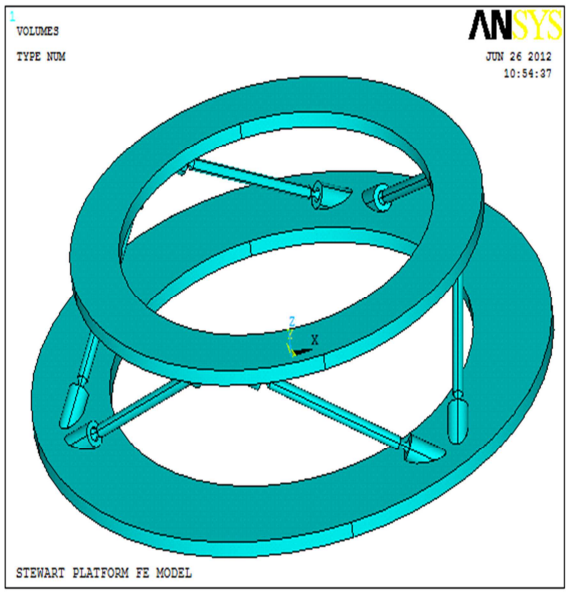

Fig. 11. Solid model of Stewart Platform with flexure joint

B. *Static Stress Analysis*

After developing the solid model in ANSYS, static analysis has been done using 3D solid element 20node186 and creating 21685 elements within the solid model and maximum number of node is 38112 within the volume of solid model. The meshed region with tetragonal element and with boundary condition is shown in “Fig. 12,” and “Fig. 13,”.

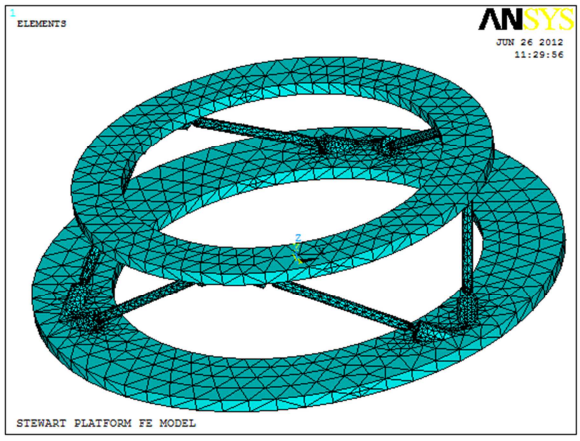

Fig. 12. Solid model with meshing

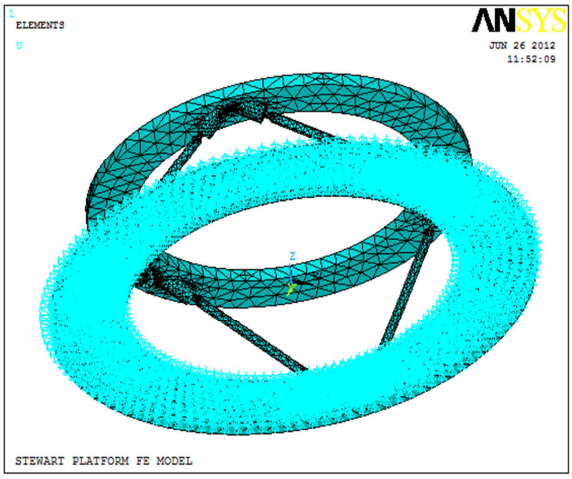

Fig. 13. Solid model with bottom plate is fixed

A payload resting on the top plate or moving plate of the Stewart Platform applying a uniform pressure at the top plate of the Stewart Platform. Due to this solid model deformed and stresses are developed in the legs. The deformed and undeformed shape after applying pressure of Stewart Platform is shown in “Fig. 14,”.

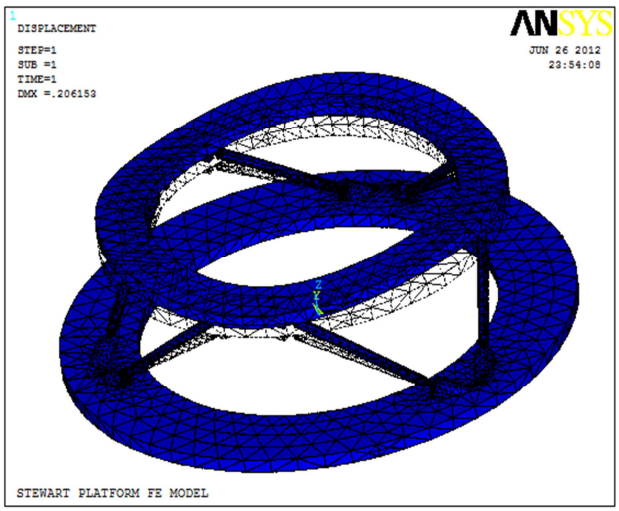

Fig. 14. Deformed and Undeformed Shape of SP

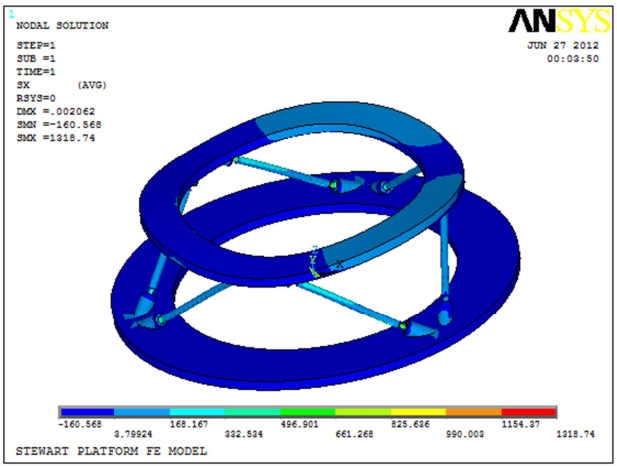

Fig. 15. Stress pattern of the X-Component in the legs

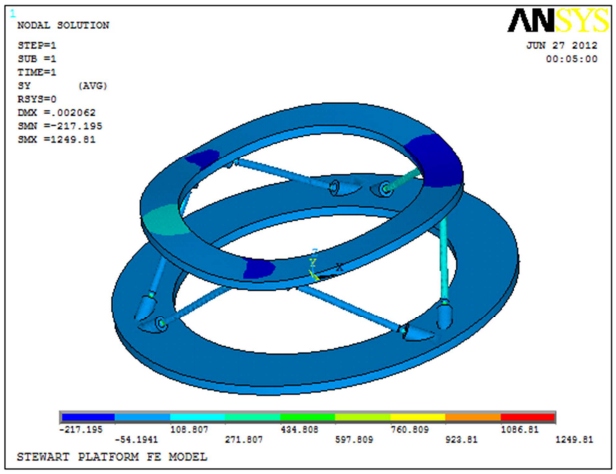

Fig. 16. Stress pattern of the Y-Component in the legs

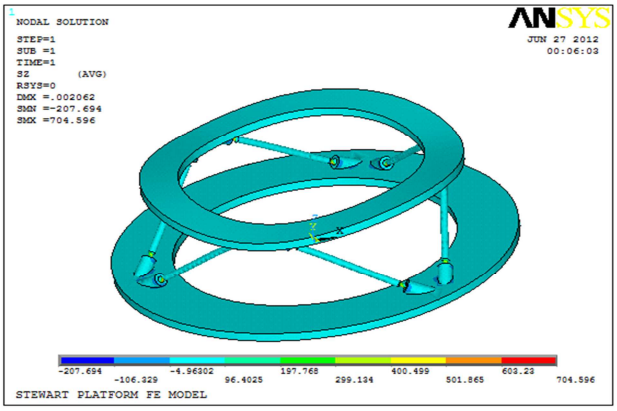

Fig. 17. Stress pattern of the Z-Component in the legs

Stresses are developed in the legs and flexure joint due to applying pressure at the top plate of SP. "Fig. 15," shows the stress pattern of the X-Component in the legs and the maximum stress is developed and has the numerical value 1318.74 N/mm^2 which is less than the Yield strength of the material. "Fig. 16," shows the stress pattern of the Y-Component in the legs and the maximum stress is developed and has the numerical value 1249.81 N/mm^2 which is less than the Yield strength of the material. "Fig. 17," shows the stress pattern of the Z-Component in the legs and the maximum stress is developed and has the numerical value 704.596 N/mm^2 which is also less than the Yield strength of the material.

C. Modal Analysis

After static analysis Modal analysis is done for the Stewart Platform in the ANSYS software. Table III shows the first five natural frequencies for the Stewart Platform.

Table III. Natural Frequency for Stewart Platform

Order	Natural Frequency (Hz)
1	177.40
2	178.29
3	345.53
4	509.72
5	511.73

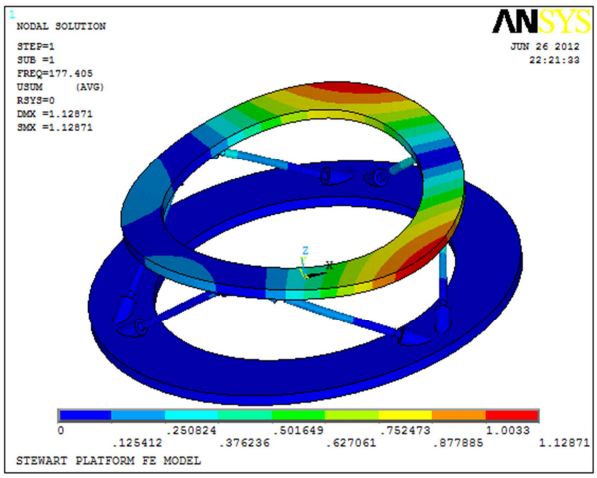

Fig. 18. The first order natural vibration mode shape

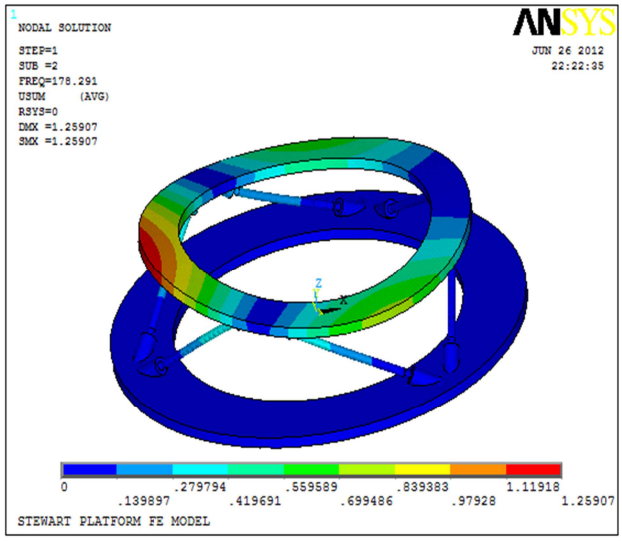

Fig. 19. The second order natural vibration mode shape

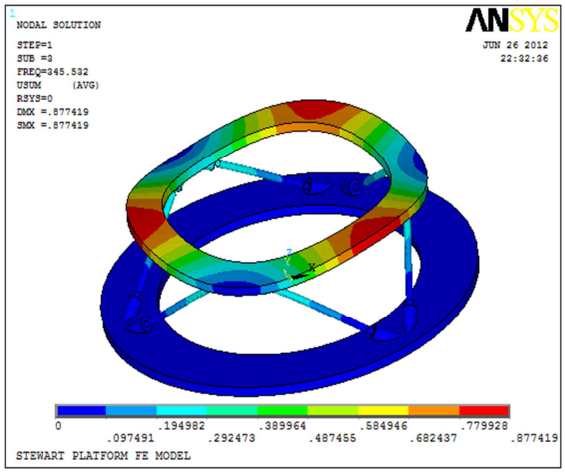

Fig. 20. The third order natural vibration mode shape

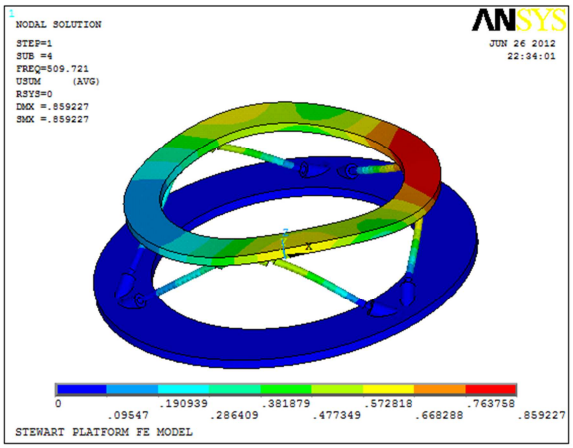

Fig. 21. The fourth order natural vibration mode shape

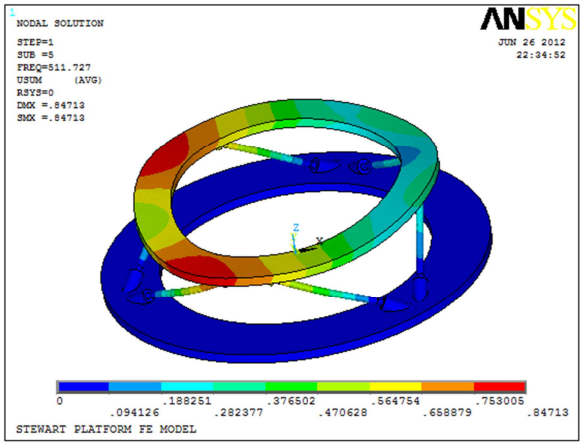

Fig. 22. The fifth order natural vibration mode shape

First five mode shapes corresponding to first five natural frequencies are shown in "Fig. 18, 19, 20, 21, and 22,".

IV. Conclusion

The main conclusions are:

1. The Hyperbolic Flexible Joint is the most accurate geometrical profile for multibody analysis.
2. The maximum stresses developed in the hyperbolic flexible joint and in the legs of the Stewart Platform are less than the material Yield strength and the structure is safe.

References

[1] L. L. Howell, "Compliant Mechanisms," New York: Wiley, 2001.

[2] S. T. Smith, "Flexures: Elements of Elastic Mechanisms," New York: Gordon and Breach, 2000.

[3] H. K. Byoung, T. W. John, G. D. Nicholas and J. G. Jason, "Analysis and Design of Parallel Mechanisms with Flexure Joints," IEEE Transactions on Robotics, vol 21, no 6, April 2004.

[4] W. Dong, Z. Du, L. Sun, "Conceptional design and kinematics modeling of a wide-range flexure hinge-based parallel manipulator," IEEE Int. Conf. on Robotics and Automation, pp. 4042-4047, Barcelona, 2005.

[5] G. M. Chen, J-Y. Jia, and Z-W. Li, "On Hybrid Flexure Hinges," IEEE Transactions on Robotics, July 2005.

[6] J. M. Paros and L. Weisbord, "How to design flexure hinges," Mech. Des. Vol. 37, pp. 151-156, Nov. 1965.

[7] T. Smith, V. G. Badami, J. S. Dale, and Y. Xu, "Elliptical flexure hinges," Rev. Sci. Instrum, vol. 68. Pp. 1474-1483, March 1997.

[8] N. Lobontiu, J. S. N. Paine, E. Garcia, M. Goldfarb, "Corner-filleted flexure hinges," ASME Trans. J. Mech. Des., vol 123, pp. 346-352, Sept. 2001.

[9] N. Lobontiu, J. S. N. Paine, E. O'Malley, M. Samuelson, "Parabolic and Hyperbolic Flexure Hinges: flexibility, motion precision and stress characterization based on compliance closed-form equations," Precis. Eng, vol. 26, 183-192, 2002.

[10] N. Lobontiu, E. Garcia, "Two-axis flexure hinges with axially-collocated and symmetric notches, Sibley School of Mechanical and Aerospace Engineering," Cornell University, 258 Upson Hall, Ithaca, NY 14850, USA, January 2003.

[11] Y. Jiantao, H. Yulei, L. Ling, Z. Yongsheng, "Analysis of a Pre-stressed Six-component Force/Torque Sensor Based on Stewart Platform," IEEE Int. Conf. on Robotics and Biomimetics, pp. 346-350, Kunming, December 2006.

[12] Dohner, J.L., Kwan, Regerlbrugge, M.E., "Active Chatter Suppression in an Octahedral Hexapod Milling Machine: A Design Study," SPIE 2721, 316–325, 1996.

[13] Nicholas Krouglicof, Luisa M. Alonso, William D. Keat, "Development of a Mechanically Coupled, Six Degree-of-Freedom Load Platform for Biomechanics and Sports Medicine," IEEE Int. Conf. on Systems, man and Cybernetics, pp. 4426-4431, 2004.

[14] T. Liu, Yoshio Inoue, Kyoko Shibata Yohei Yamaski, Masafumi Nakahama, "A Six-Dimension Parallel Force Sensor for Human Dynamics Analysis," IEEE Int. Conf. on Robotics, Automation and Mechatronics, Singapore, pp. 208-212, December 2004.

[15] J. Zhao, X. Y. Wang, L. Zhang, H. G. Cai, "Finite Element Analysis of Six-Dimension Stiff Force/Torque Sensor Elastomer for Robots," Int. Symposium on Instrumentation Science and Technology, Jinan, China, Aug. 18-22, 2002.

[16] Akhlaq, A., "Modeling and Simulation of a Multi-Axis Active Vibration Isolation based on S-G Mechanism," M.Tech Thesis, Dept. of Mechanical Engg., ZHCET, AMU, Aligarh, 2011.